Variation of through-culm wall morphology in P. edulis bamboo strips used in glue-laminated

bamboo beams

Yusuf Akinbade¹, Kent A. Harries², Bhavna Sharma³ and Michael H. Ramage⁴

Abstract

Image analysis is used to quantify the distribution of fibre volume ratio, V₆ in strips of P. edulis bamboo

obtained from two commercially available glue-laminated bamboo beam products. In total, 58 cross

sections containing more than 3500 19 x 6 mm strips were analysed. Simple digital manipulation

techniques were found to work well in establishing fibre volume data from the 1200 dpi source images.

Total fibre volume for each strip was established and was found to vary in a linear manner through the

strip thickness. The observations presented indicate significantly different bamboo source (feedstock)

material used by the two manufacturers. Autocorrelation analysis was used to demonstrate that the

orientation of the individual strips in each beam section was not random. The impact of a non-random

distribution of strip orientation in a section subject to flexure is relatively small but does result in

variation from analyses that assume a homogenous distribution of mechanical properties. Finally, nodes, a

weak location in glued-laminated bamboo members were observed to represent 3 to 4% of all strips in a

given cross section. The distribution of nodes appeared to be random.

Keywords

bamboo; fibre volume ratio; glue-laminated bamboo lumber; image analysis

¹ Doctoral Candidate, University of Pittsburgh

² Professor, University of Pittsburgh, kharries@pitt.edu (corresponding author)

³ Assistant Professor, University of Southern California

⁴ University Reader, Cambridge University

Introduction

Engineered bamboo products, including glue-laminated bamboo, are becoming recognised as a viable load-bearing structural material in construction applications (Sharma et al. 2015a). In glue-laminated bamboo products, strips of green bamboo are planed to desired dimensions and treated. Strips are either hot- or cold pressed into a board product and the boards further assembled into prismatic structural members (Liu et al. 2016). While many studies have investigated the behaviour of laminated bamboo, none, to the authors' knowledge, have specifically investigated the nature of the constituent bamboo strips – the feedstock, as it were – used to fabricate the glue-laminated bamboo. In particular, the expected variability inherent in the use of a natural material should certainly be of interest to manufacturers of these products.

At the same time, in the realm of modelling bamboo material behaviour, it is necessary to understand the uncertainty inherent in ascribing material properties to a natural material (Harries et al. 2019a). As a natural material, measured mechanical properties of bamboo are highly variable (coefficients of variation for many standard test methods are routinely reported on the order of 20 to 30%). Assessing the impact of this uncertainty on the calibration of design equations will be critical if bamboo is to gain acceptance as a load-bearing structural engineering material. An approach to modelling bamboo by applying a random fields approach (Alder and Taylor 2010) to a scale-independent functionally-graded material (FGM) model as means of modelling uncertainty in full-culm bamboo behaviour has been proposed (Harries 2016) and is presently being investigated (Harries et al. 2019; Akinbade 2019). Although not the focus of this paper, it is necessary to obtain and quantify relatively large amounts of data on both natural variation and spatial dependency of bamboo properties. Laminated bamboo materials provide an opportunity to investigate large data sets of individual culm wall data. At a minimum, the material in a given glue-laminated member will be from the same species and, in most cases, from the same batch of bamboo. This provides some control for assessing statistical variation of properties within a relatively large batch size.

This study uses image analysis to quantify the distribution of fibre volume ratio, V_f , in strips of *Phyllostachys edulis* bamboo used in commercially available glue-laminated bamboo beams. The distribution and implications of strip orientation in a cross section is also addressed.

Bamboo Morphology

The structure of bamboo, shown in Figure 1, is composed of culms (stalks) with solid transverse diaphragms or 'nodes' separating hollow inter-nodal regions along its height. The circular cross section (Figure 1b) is composed of vascular bundles oriented parallel to the culm's longitudinal axis embedded in a parenchyma tissue matrix (Grosser and Liese 1971). The vascular bundles (Figure 1d) contain unidirectional cellulosic fibres which are the primary source of the bamboo's longitudinal strength. The fibres surround vessels: voids in the section that carry water vertically through the plant when it is living. As seen in Figure 1c, the density of fibres increases from the inner culm wall to the outer culm wall. Like any fibre-reinforced material, mechanical properties are highly correlated to the proportion and distribution of fibres in the cross section. Mechanical properties are influenced by density, which depends on fibre content, fibre diameter, and cell wall thickness (Janssen 2000). The volume fraction of fibres ranges from approximately 60% at the exterior face of the culm wall to 10-15% near the interior face (Figure 1c). The variation in density through the culm wall has been assumed by various researchers to be linear, quadratic, exponential, or a power function and is known to be species-dependent (Amada et al. 1996). Based on a rule-of-mixtures approach, the longitudinal modulus of a bamboo strip is proportional to the fibre volume, V_{ℓ} (Akinbade et al., 2019).

High Resolution Images of Glue-laminated Bamboo Beams

High resolution images of cross sections of 58 glue-laminated bamboo beams were obtained. The images, originally reported by Penellum et al. (2018), are 1200 dpi scans of the cross sections; an example is shown in Figure 2a. The commercially produced beams – representing material obtained from two different manufacturers (designated batches M and P) – had been previously tested in flexure, as reported in a number of studies (Sharma et al. 2015a, 2015b and 2017). All material was *P. edulis* (Moso) bamboo originating in China. The beams were fabricated from 19 mm thick boards, with each board made of

bamboo strips 19 mm wide and 6 mm thick in the direction through the culm wall (Figure 3). The overall thickness of the source material culm wall is unknown however in typical practice, 6 mm strips are taken from culms having a wall thickness on the order of 8 to 10 mm. The strips are therefore taken from the middle region of the culm wall as shown in Figure 3. Image analysis of the full beam sections having the objective of determining the applicability of composite theory (i.e., rule of mixtures) to the glue-laminated members is reported by Penellum et al. who determined the fibre volume ratio, V_f , of the gross beam cross sections for both batches to be 0.21 (COV = 0.05).

Image Extraction

Over 3500 individual images of the 19 x 6 mm strips (Figure 2b) were extracted from the 58 beam section images available (Table 1). Each image is approximately 900 x 300 pixels resulting in a pixel resolution of approximately 2400 pixels/mm². Following visual screening, approximately 13% of the extracted images were excluded from analysis due primarily to poor image quality or features unsuited to image analysis. Examples of excluded images are shown in Figures 2d-e. Additionally, approximately 3.5% of the strip sections were near the bamboo nodal region (Table 1 and Figure 2c). The varying fibre orientation and bamboo morphology in this region (Liese 1998) is also unsuitable for the analysis conducted and these strips were excluded from analysis. Following analyses of the remaining 2929 images (see below), 19 outliers determined using the interquartile rule were also excluded from further analysis – these outliers were attributed to additional anomalies affecting image analysis which were not identified in the initial visual screening.

Image Analysis

Using a purpose-written MatLab script (Akinbade 2019), based on image contrast, each image (Figure 4a) was processed to produce a high contrast image allowing differentiation of the bamboo fibre bundles as seen in Figure 4b. The contrast imaging was able to discriminate between fibre bundle and vessels, excluding the latter from the vascular bundle. As a result, the fibre volume ratio, V_r is correctly reported. In some other studies, larger fibre volume ratios are reported; these are thought to also include the vessels contained within the vascular bundle and therefore over-report the value of V_t . Using the MatLab script,

each full culm wall thickness image was divided into ten equal sub images in the through-culm wall (6 mm) direction (Figure 4). The fibre components were extracted from the images based on contrast (Figure 4b) and the fibre volume ratio determined for each sub image. From this analysis the total fibre volume ratio of each strip, V_f and the distribution as a function of location in the strip can be determined. Figure 5 shows examples of data obtained for M and P strips. In each image, 100 randomly selected fibre volume distributions are shown; the heavy black line indicates the average value obtained from all analysed strips. Total fibre volume ratio, V_f , obtained from this analysis is given in Table 1. The values are different than those reported by Penellum et al. (2018) The differences are an artefact of the different image analysis algorithms used. This highlights an important aspect of similar digital analysis: that results and/or interpretation provided by different algorithms will vary. Therefore, comparisons relying on such image data must be internally consistent; that is, data must be collected using the same algorithm. A second reason for the difference is that Penellum et al. imaged the entire beam (i.e., Figure 2a) without excluding portions of the image that were unclear or contained nodal regions.

Distribution of fibre volume ratio through the culm wall thickness is not meaningful since the actual location of the 6 mm sample within the culm wall is unknown. Nonetheless, the nature of the distribution and its variation is a measure of the uncertainty inherent in ascribing geometric or material properties to bamboo. Each acquired fibre distribution was fitted to a linear relationship as described by Eq 1.

$$V_f = mx + b$$
 Eq. 1

The value of m describes the variation of the fibre volume through the strip dimension x which ranges from 0 to 6 mm (see Figure 3). The value b is a function of the location of the 6 mm strip within the culm wall and is therefore not uniquely defined in this study. The values of m and b determined from regression analyses are given in Table 1. Additionally, the mean relative error (MRE) of Equation 1 is shown. The statistical distributions of V_f and parameters, m and b, can be shown (with a confidence of 95%) to be normal (Figure 6).

A linear fit function was selected since this has been reported in the literature (Janssen 1981). Exponential (Nogata and Takahasi 1995; Amada et al. 1996) fit functions were also obtained that yielded essentially

identical MRE values; the discussion therefore considers only the simpler linear distribution. Others have reported polynomial distributions (Ghavami et al. 2003; Ghavami and Marhinho 2005; Akinbade et al. 2019) across the full culm wall. The strips considered represent only a part of the culm wall thickness and exclude both the extreme outer and inner fibres (see Figure 3); it is these regions that often require a higher order polynomial distribution to be used (Akinbade et al. 2019). The authors considered polynomial distributions, however these were no better than linear distributions across the range of data obtained.

In situ Bamboo Strip Orientation

Table 2 summarises the data obtained for the typical Batch M section shown in Figure 2a. In Table 2, the values of V_f and m (from Eq. 1) are shown. Additionally, an arrow indicates the orientation of each strip comprising the section. Initial observation suggested that the distribution of strip orientation was not random as might be expected; this hypothesis was tested as follows.

Strip orientation was coded in a binary fashion and autocorrelation tests (NIST 2019) were conducted; results are presented in Table 1 and representative autocorrelation plots are shown in Figure 7. For an autocorrelation test, RhI is the auto correlation at lag = 1 and $y_{0.95}$ is the 95% confidence limit for test which is a function of the number of strips in each beam. A result of $RhI/y_{0.95} < 1$ indicates that the sample has a random distribution; $RhI/y_{0.95} \ge 1$ indicates a non-random distribution. Results indicate that all P Batch beams exhibit a non-random distribution of strip orientation and 30 of 38 Batch M beams exhibit non-random distribution. These results were additionally confirmed using 'runs tests' (NIST 2019). In Figure 7, two representative cases from Batch M are shown: one for a sample that exhibited distinctly non-random distribution ($RhI/y_{0.95} = 2.98$) and a second exhibiting essentially random distribution ($RhI/y_{0.95} = 0.15$).

There is evidence of periodicity to the autocorrelation of the orientation distribution, particularly in those specimens exhibiting non-random distribution (Figure 7a). The period corresponds to the number of bamboo strips comprising the 'depth' of the beam (using the orientation shown in Table 2). It is hypothesised that this periodicity results from the beam assembly process in which the strips are

assembled into 19 mm wide 'boards' (the vertical columns in Table 2) which are subsequently assembled into the wider beams (Sharma et al 2015a).

For the autocorrelation presented in Table 1 and Figure 7a, all beams were coded in the 'vertical' orientation shown from the top to bottom followed by left to right of the image (Figure 7b). To test the hypothesis that the periodicity may arise from the assembly process, the same beams were recoded 'horizontally' from left to right then top to bottom (Figure 7d); the results are shown in Figure 7c. While the conclusions of non-random and random distributions remain the same (as expected), there is no apparent periodicity in the same non-random beam coded horizontally. Instead the autocorrelation indicates a strongly autoregressive behaviour. The apparently non-random distribution is an artefact of the laminated bamboo beam production process.

Effect of bamboo strip orientation

An advantage of engineered products such as glue-laminated bamboo is that amalgamation of smaller constituent elements in an essentially random fashion mitigates the variation of flaws (e.g. nodes, defects) in the individual constituents. For example, reported values of compression, shear and flexural properties of glue-laminated bamboo beams typically exhibit coefficients of variation (COV) less than 10%, tension properties exhibit a higher COV, approaching 20%, due to the inclusion of nodes in such engineered products (e.g., Sharma et al. 2015b). The "raw" bamboo feedstock, on the other hand, typically exhibits COV values on the order of 20% even within batches having good quality control (e.g., Akinbade et al. 2019).

A non-random distribution of bamboo orientation could affect physical properties of the beam including its flexural and shear capacity, and long-term creep-related performance. The following identifies these effects in a conceptual manner using an idealised prototype beam 10 strips (60 mm) deep by 1 strip (19 mm) wide (Figure 8). Batch M strips are assumed in this hypothetical example. Based on the application of the rule-of-mixtures in the longitudinal direction (confirmed by Akinbade et al. 2019 and Penellum et al. 2018), each strip is assumed to have a distribution of tensile and compression modulus proportional to the average distribution of fibre volume ratio reported in Table 1; that is:

With x ranging from 0 to 6 mm, the ratio of moduli at the strip edges is $E_{max}/E_{min} \approx 2$. In Figure 8 the stress distribution for four cases each having the same linear strain distribution are shown.

In case a, each strip is assigned a single value of modulus (no gradient) equal to the average modulus calculated using Eq. 2. The resulting stress distribution (Figure 8a) is linear and the resulting section moment capacity corresponding to the strain distribution selected is assigned the value M_0 . Case a would typically be used in design where the modulus is determined from strip bending tests (ASTM D7264 or similar). The remaining cases assign the linear gradient of modulus defined by Equation 2 to each strip. Cases b and c represent cases in which the individual orientation of each strip (shown in Figure 8) is 'optimised' to maximise or minimise the section moment capacity, respectively. These cases are both distinctly non-random distributions of orientation. The corresponding section capacities are $1.04M_0$ and $0.96M_0$, respectively. Finally, case d is one example of a random distribution (created using RAND function in Excel). In this case the section moment capacity is $1.01M_0$. Other random cases vary between cases b and c. In each of cases b - d, the variation from M_0 is inversely proportional to overall beam depth (number of strips); that is, shallower members will see a greater effect from non-random distribution of orientation. Finally, the variation from M_0 is proportional to the ratio E_{max}/E_{min} ; that is, a steeper fibre gradient in individual strips will result in greater variation in section capacity.

For the four cases shown, the extreme compression (ε_C) and tensile (ε_T) strains have equal magnitude, placing the neutral axis of the beam at one half the beam depth. Based on the combination of strip orientations possible, the neutral axis may vary a small amount: about 1% for the ten-strip example shown. This variation is also inversely proportional to beam depth and proportional to E_{max}/E_{min} .

A second issue evident in the stress distributions shown in Figure 8 is the stress raiser associated with strips that are bonded outer culm wall-to-inner culm wall (O-I). Clearly, this effect cannot be avoided entirely, but a random distribution of strip orientation, especially over a member that is multiple strips wide, should mitigate this stress raising effect. Longitudinal shear failure along the bond lines of glue-laminated bamboo members in flexure are commonly observed in laboratory studies (i.e., Sharma et al.

2015a). Limited (and occasionally contradictory) data suggests that the bond between two inner culm walls (I-I) is superior to that between two outer culm walls (O-O), The O-I condition falls closer to the better I-I condition (Chaowana et al. 2015; Li et al. 2015; Zeng et al. 2019). The reason for the difference is the inherent wettability of the bonded faces, which is also affected by surface preparation during fabrication (Sharma et al. 2018, Sharma and van der Vegte 2019).

Finally, long-term creep distortion of bamboo strips has been shown to be affected by the orientation of the strip – whether the outer culm wall is in compression or tension. Creep deformations are greater and residual capacity is reduced for single strip specimens are loaded such that their fibre-rich outer culm wall is in tension (Gottron et al. 2014). The reason for this behaviour is that tensile damage associated with sustained loads to the fibre-rich outer culm wall is mostly non-recoverable. Conversely, similar compression damage to the inner culm wall is mostly recoverable.

Presence of Nodes

As shown in Table 1, in all of the 58 cross sections (containing 3517 strips) analysed, 3 to 4% of the strips were identified as nodal regions (Figure 2c) at the cross section investigated (three nodes are seen in the 68-strip section shown in Figure 2a – these are identified in Table 2). The occurrence of nodes in glue-laminated members is primarily a function of the internode length of the bamboo being used. A longer internode length will result in fewer nodes occurring at a given cross section of a glue-laminated member. Anecdotally, the presence of nodes in the 58 sections in this study appeared to be random – there is no way, however, to test this hypothesis.

In a glue-laminated member, nodes primarily affect tensile and flexure-induced tensile behaviour. In bamboo, the presence of a node has little effect on compressive capacity or modulus (Gauss et al. 2019). However, in tension, a strip containing a node will have a strength about one-third that of the internode region and a modulus about two-thirds of the internode region (Gauss et al. 2019).

Conclusion

This study used image analysis to quantify the distribution of fibre volume ratio, V_f , in strips of P. edulis bamboo obtained from two commercially available glue-laminated bamboo beam products. In total, 58

cross sections containing more than 3500 19 x 6 mm strips were analysed. Simple digital manipulation techniques were found to work well in establishing fibre volume data from the 1200 dpi source images. Although all bamboo was Chinese P. edulis, variation was observed: the measured fibre volume ratio for each strip was 0.23 for Batch M and 0.19 for Batch P; the coefficient of variation observed was 12% and 19%, respectively. Both batches could be modelled as having a linear distribution of V_f through their thickness although the gradient was different in each case: 0.025/mm and 0.032/mm for Batch M and P, respectively. These observations indicate significantly different bamboo source (feedstock) material for the two batches. Indeed, many factors may affect the properties of strips used even by the same manufacturer. Bamboo suppliers, harvest conditions, and location of strips along culm all may result in variation of strip properties.

Using an autocorrelation analysis, it was demonstrated that the orientation of the individual strips in each beam section was not random as might be expected for a glue-laminated product. The impact of a non-random distribution of strip orientation in a section subject to flexure is relatively small but does result in variation from analyses that assume a homogenous distribution of mechanical properties. The degree of variation from the homogenous assumption is inversely proportion to beam depth (number of strips) and proportional to the gradient of V_f . Nodes, a weak location in glued-laminated members, were observed to represent 3 to 4% of all strips in a given cross section. The distribution of nodes appeared to be random. The findings of this study can be considered by the engineered bamboo community in the development of quality control/quality assurance (QC/QA) and grading protocols. Penellum et al. (2018) illustrated that modelling glue-laminated bamboo using fibre-reinforced composite approach (i.e., using rule-of-mixtures) is appropriate. The image analysis approach reported in this study illustrates a relatively simple method for obtaining the necessary fibre volume ratio and distribution data, including the need to exclude portions of the image from analysis. Furthermore, the study provides an indication of the variation present in commercially available glue-laminated bamboo beams.

Acknowledgements

This research was supported through [US] National Science Foundation Award 1634739 *Collaborative Research: Full-culm Bamboo as a Full-fledged Engineering Material*. The original images were generated through support of a Leverhulme Trust Programme Grant and the [UK] Engineering and Physical Sciences Research Council (EPSRC Grant EP/K023403/1).

References

Akinbade, Y. (2019) *Mechanical Characterization of Full-Culm Bamboo*, PhD Dissertation, University of Pittsburgh (in process)

Akinbade, Y., Harries, K.A., Flower, C., Nettleship, I., Papadopoulos, C., and Platt, S.P. (2019) *Through-Culm Wall Mechanical Behaviour of Bamboo*, Construction and Building Materials, **216**, 485-495.

Alder, R.J. and Taylor, J.E. (2010) *Random Fields and Geometry*, Springer Monographs in Mathematics, New York.

Amada, S., Munekata, T., Nagase, Y., Ichikawa, Y., Kirigai, A. and Zhifei, Y. (1996) The mechanical structures of bamboos in viewpoint of functionally gradient and composite materials, *Journal of Composite Materials*, **30**, 800-819.

ASTM D7264 – 15 Standard Test Method for Flexural Properties of Polymer Matrix Composite Materials, ASTM International, West Conshohocken PA USA.

Chaowana, P., Jindawong, K., Sungkaew, S. (2015) Adhesion and Bonding Performance of Laminated Bamboo Lumber made from *Dendrocalamus sericeus*. *Proceedings of the 10th World Bamboo Congress*, Korea.

Gauss, C., Harries, K.A. and Savastano, H. (2019) Use of ISO 22157 Mechanical Test Methods and the Characterisation of Brazilian *P. edulis* bamboo, *Construction and Building Materials*, **228**, 116728.

Ghavami, K. and Marinho, A.B. (2005) Propriedades físicas e mecânicas do colmo inteiro do bambu da espécie *Guadua angustifolia* [Physical and mechanical properties of the entire culm of the bamboo species *Guadua angustifolia*], *Revista Brasileira de Engenharia Agrícola e Ambiental* **9**(1) 107-114. (in Portuguese)

Ghavami, K., Rodriques, C.S., and Paciornik, S., (2003) Bamboo: Functionally Graded Composite Material, *Asian Journal of Civil Engineering (Building and Housing)* **4**(1) 1-10.

Gottron, J. Harries, K. and Xu, Q. (2014) Creep Behaviour of Bamboo, *Journal of Construction and Building Materials*, **66**, 79–88.

Grosser, D. and Liese, W. (1971) On the anatomy of Asian Bamboos, with Special Reference to their vascular bundles. *Wood Science and Technology*, **5**, 290-312.

Harries, K.A., Nettleship, I., Akinbade, Y., Papadopoulos, C., Acosta, F., Morales Albino, J. and Ariezaga Gonzalez, M. (2019) Full-culm Bamboo as a Full-fledged Engineering Material, *18th International Conference on Non-Conventional Materials and Technologies* (18NOCMAT) Nairobi, Kenya, July 2019

Harries, K.A. (2016) *Full-culm Bamboo as a Full-fledged Engineering Material*, National Science Foundation Proposal, Award Number 1634739,

www.nsf.gov/awardsearch/showAward?AWD ID=1634739 [20 June 2019]

Janssen, J. (1981) *Bamboo in Building Structures*. Doctoral Dissertation, Eindhoven University of Technology, Netherlands.

Janssen, J.J.A., (2000) *Designing and Building with Bamboo*, INBAR Technical Report 20. International Network for Bamboo and Rattan, Beijing, China.

Li, T., Cheng, D., Walinder, M.E.P. and Zhou, D.G. (2015) Wettability of oil heat-treated bamboo and bonding strength of laminated bamboo board. *Industrial Crops and Products*, **69**, 15-20.

Liese, W., (1998) The Anatomy of Bamboo Culms, Brill, 204 pp.

Liu, X., Smith, G.D., Jiang, Z., Bock, M.C.D., Boeck, F., Frith, O., Gatóo, A., Liu, K., Mulligan, H., Semple, K.E., Sharma, B. and Ramage, M. (2016) Nomenclature for Engineered Bamboo. *BioResources*, 11(1), 1141-1161.

NIST (2019) *NIST/SEMATECH e-Handbook of Statistical Methods*, http://www.itl.nist.gov/div898/handbook/ [27 February 2019].

Nogata, F. and Takahashi, H. (1995) Intelligent functionally graded material: bamboo, *Composites Engineering* **5**, 743-751.

Penellum, A., Sharma, B., Shah, D.U., Foster, R.M. and Ramage, M.H. (2018) Relationship of structure and stiffness in laminated bamboo composites. *Construction and Building Materials* **165**, 241-246

Sharma, B., Gatoo, A., Bock, M. and Ramage, M.H. (2015a) Engineered bamboo for structural applications, *Construction and Building Materials* **81**, 66–73.

Sharma, B., Gatoo, A. and Ramage, M.H. (2015b) Effects of processing methods on the mechanical properties of engineered bamboo, *Construction and Building Materials* **83**, 95–101.

Sharma, B., Bauer, H. and Schickhofer, G. and M.H. Ramage (2017) Mechanical characterization of structural laminated bamboo, *ICE Structures B* **170** (4), 250–264.

Sharma, B., Shah, D.U., Beaugrand, J., Janecek, E.R., Scherman, O.A., Ramage, M.H. (2018) Chemical composition of processed bamboo for structural applications, *Cellulose* **25**, 3255-3266.

Sharma, B. and van der Vegte, A. (2019) Chapter 21: Engineered Bamboo for Structural Applications in *Nonconventional and Vernacular Construction Materials: Characterisation, Properties and Applications*, 2nd edition. K.A. Harries and B. Sharma, editors. Woodhead (Elsevier) Publishing Series in Civil and Structural Engineering

Zeng, Q., Zhang, Q., Lu, Q., Zhou, Y., Chen, N., Rao, J. and Fan, M. (2019) Wetting behavior and laminate bonding performance of profiled tangential surfaces of moso bamboo, *Industrial Crops and Products*. (in press).

Table 1 Summary of image analysis and autocorrelation test (COV in parentheses).

	Ba	tch	M	P	
	beam dime	nsion (mm)	140 x 90	120 x 60	
image analysis	number	of beams	38	20	
	19 x 6 mm s	trips in beam	64 or 78	48 or 54	
	strips e	xtracted	2590	927	
of fibre	strips a	nalyzed	2309 of 2590	601 of 907	
volume	near-node strips		80 of 2590	37 of 907	
distribution	fibre volur	ne ratio, V_f	0.234 (0.12)	0.190 (0.19)	
		m (mm ⁻¹)	0.025 (0.29)	0.032 (0.24)	
	$V_f = mx + b$	b	0.160 (0.21)	0.094 (0.46)	
		MRE	0.125	0.214	
autocorrelation test of strip orientation	beams having random distribution		8 of 38	0 of 20	
	$(Rh1/y_{0.95} < 1.0)$		8 01 38		
	$low Rh1/y_{0.95}$		0.15	1.53	
	high <i>Rh1/y_{0.95}</i>		3.15	2.70	

Table 2 Distribution of strip properties in one Batch M cross section.

Secretary Commence of the Comm	0.267 0.024	•	0.283 0.038	•	0.243 0.030	ullet	nd	•
	0.290	Ψ	0.222	Ŧ	0.246	_	0.279	+
	0.033	0.024	•	0.023	↑	0.038	•	
Marie Committee of the	0.257	F	0.243	4	0.279	+	0.241	4
approximate and the second sec	0.029		0.038		0.029		0.026	•
The second secon	0.180 0.031	•	no data	•	0.231 0.015	•	0.262 0.018	•
	0.254	4	0.287	+	0.248	+	0.259	4
	0.014		0.027		0.021		0.026	_
According to the State of the Control of the Contro	0.208 0.036	•	0.212 0.023	↑	node		0.199 0.029	↑
	0.210	Ψ	0.219	_	0.254	Ψ	0.249	_
	0.025		0.032	↑	0.028	•	0.039	↑
	0.261 0.033	•	0.226 0.016	•	0.242 0.013	↑	0.232 0.029	→
Briefergas Lauge (Capacida)	no data	1	0.239	Ψ	0.235	Ψ	0.204	4
	no data	1	0.020		0.026		0.018	
	no data	↑	0.232 0.028	¥	0.178 0.026	↑	0.168 0.029	•
	0.269	1	node		0.245	↑	0.229	+
Paramana and American and Ameri	0.014	Т			0.029	Т	0.018	•
	0.279 0.021	↑	0.270 0.017	•	0.214 0.026	↑	no data	↑
- TTS 3 9 3 7 5 1	0.241 0.031	↑	no data		no data	_↑	-110 data	+
		`	node		0.239	↑	0.226	←
					0.022		0.025	•
And the second of the second o	0.204 0.033	↑	0.248 0.025	ullet	0.182 0.019	↑	0.249 0.028	↑
	0.033		0.023		0.019		0.028	
	0.041	↑	0.029	↑	0.028	↑	0.033	↑
mananamanamanamanamanamanamanamanamanam	0.264	1	no data	1	0.252	_	0.246	+
	0.008	不		T	0.035	↑	0.030	•
	LEGEND:		$V_f \ m$	↑	arrow points toward outer culm wall			
	L		m		outer cumi wan			

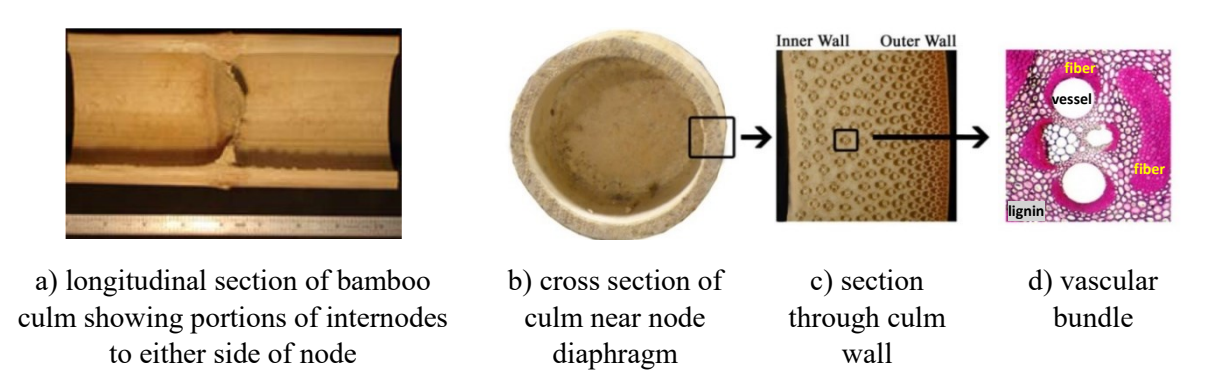
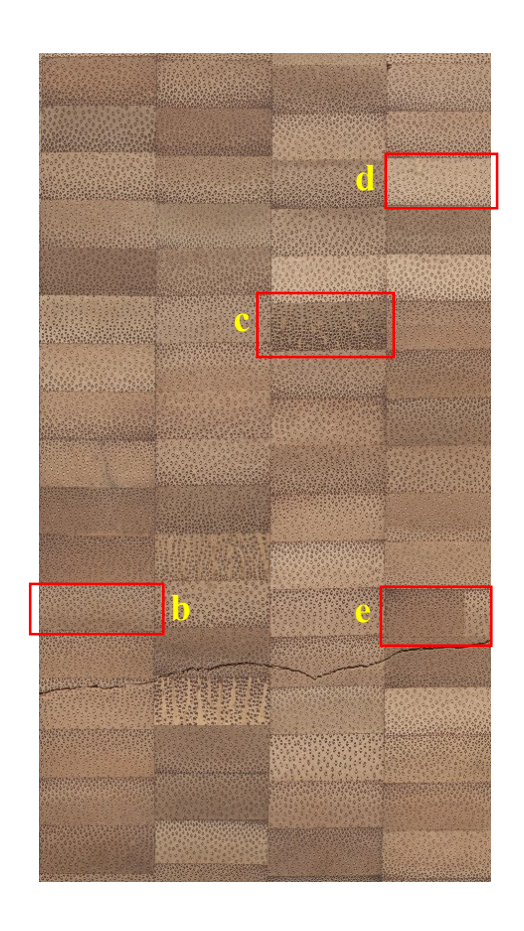
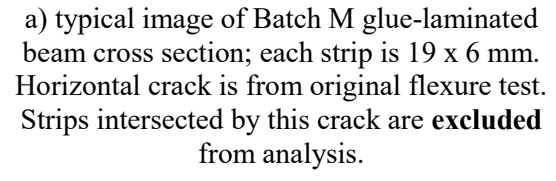


Figure 1 Anatomy of bamboo culm showing functionally graded distribution of fibre in culm wall (Akinbade et al. 2019)







b) typical strip image used for analysis



c) near-node strip section excluded from analysis



d) incomplete strip – likely due to cutting/polishing beam section **excluded** from analysis



e) other anomalies **excluded** from analysis, in this case a strip composed of two smaller glued strips

Figure 2 Glue-laminated bamboo beam and individuals strips extracted for image analysis.

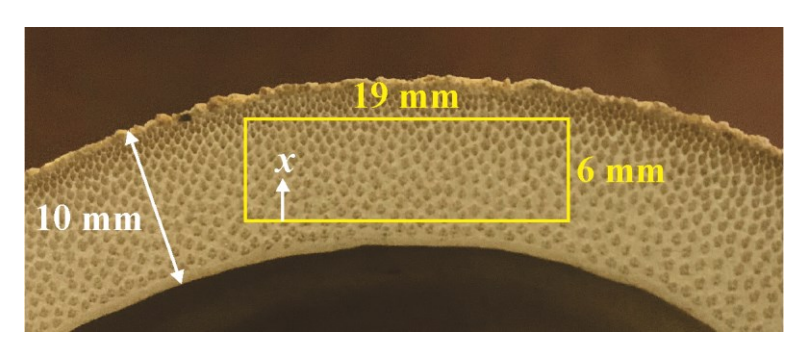


Figure 3 Image of strip location in a typical culm wall cross-section.

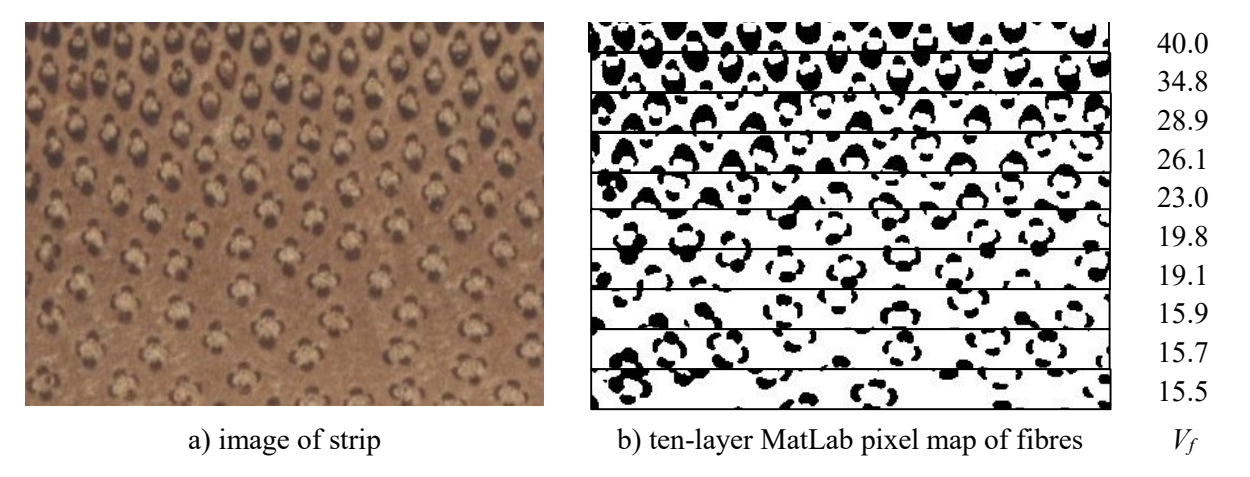
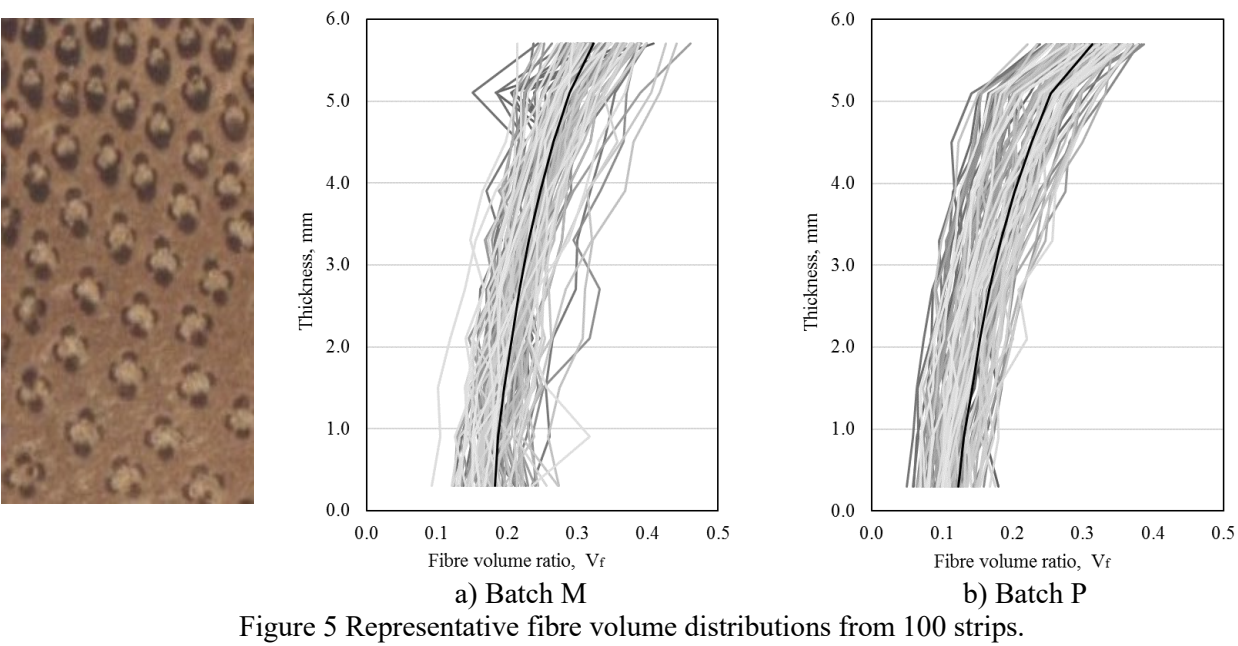


Figure 4 Example of digital image analysis of 6 mm thick strip (19 mm dimension cropped in this figure).



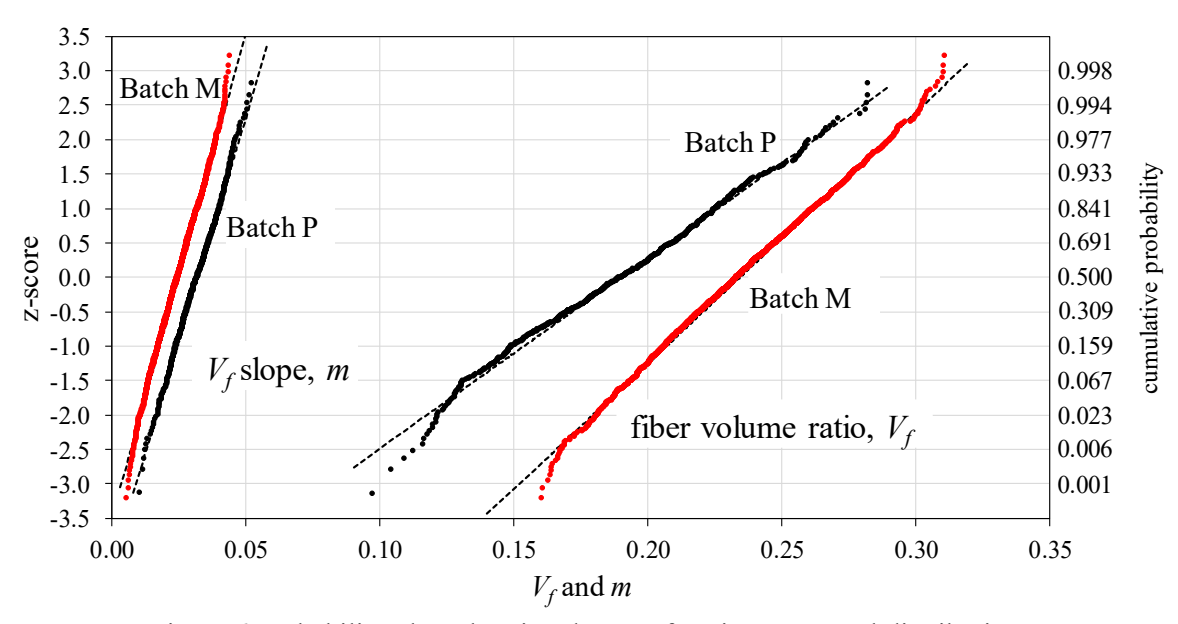


Figure 6 Probability plots showing data conforming to normal distribution.

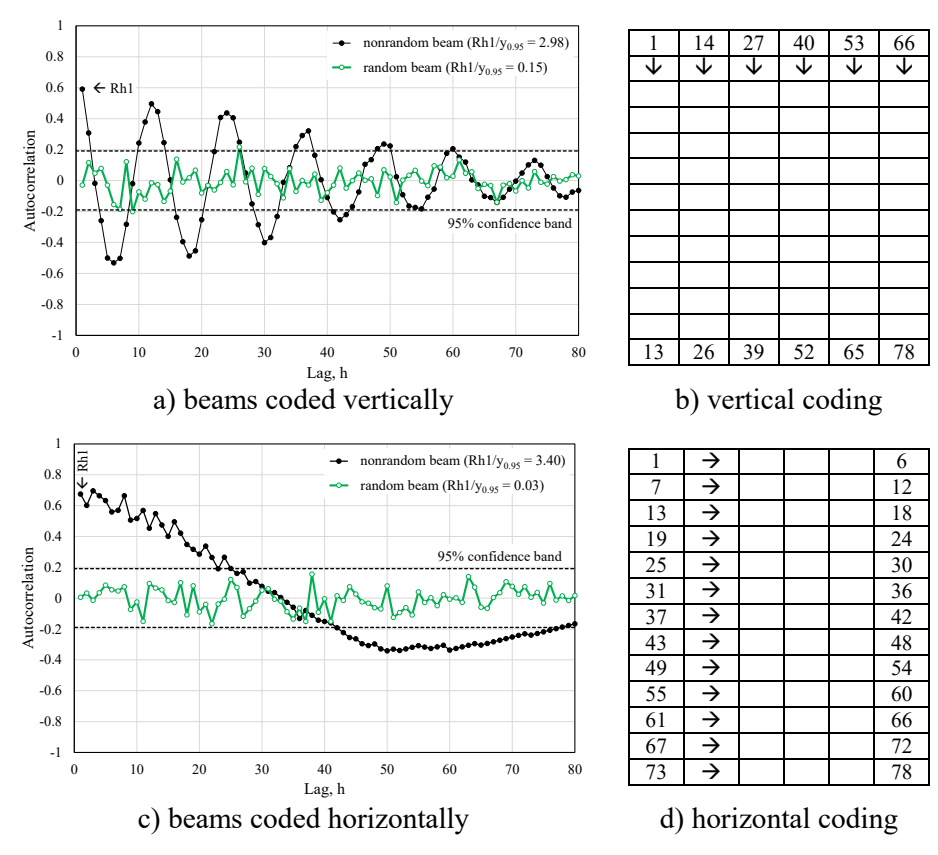


Figure 7 Representative autocorrelation plots illustrating range of results.

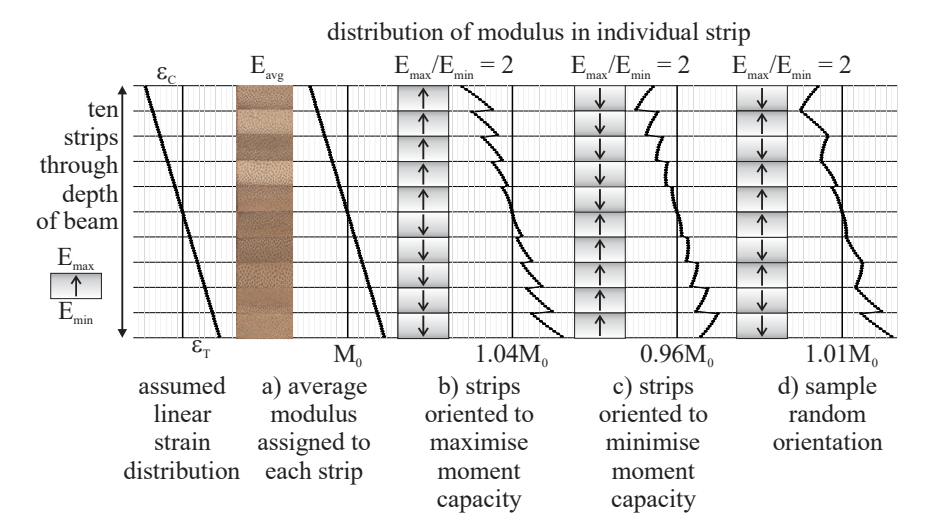


Figure 8 Effect of strip orientation on flexural stress distribution of glue-laminated beam